

Dielectric properties of spark plasma sintered AlN/SiC composite ceramics

Peng Gao, Cheng-chang Jia, Wen-bin Cao, Cong-cong Wang, Dong Liang, and Guo-liang Xu

School of Materials Science and Engineering, University of Science and Technology Beijing, Beijing 100083, China

(Received: 7 October 2013; revised: 23 December 2013; accepted: 26 January 2014)

Abstract: In this study, we have investigated how the dielectric loss tangent and permittivity of AlN ceramics are affected by factors such as powder mixing methods, milling time, sintering temperature, and the addition of a second conductive phase. All ceramic samples were prepared by spark plasma sintering (SPS) under a pressure of 30 MPa. AlN composite ceramics sintered with 30wt%–40wt% SiC at 1600°C for 5 min exhibited the best dielectric loss tangent, which is greater than 0.3. In addition to AlN and β -SiC, the samples also contained 2H-SiC and Fe₅Si₃, as detected by X-ray diffraction (XRD). The relative densities of the sintered ceramics were higher than 93%. Experimental results indicate that nano-SiC has a strong capability of absorbing electromagnetic waves. The dielectric constant and dielectric loss of AlN-SiC ceramics with the same content of SiC decreased as the frequency of electromagnetic waves increased from 1 kHz to 1 MHz.

Keywords: ceramic materials; composite materials; aluminum nitride; silicon carbide; spark plasma sintering; dielectric losses

1. Introduction

Trends in electronic device manufacturing and applications indicate that substrates having high thermal conductivities will become more important [1]. Aluminum nitride is a promising substrate and packaging material for high-power integrated circuits because of its high thermal conductivity, low dielectric constant, high electrical resistivity and thermal expansion coefficient, which are similar to the properties of silicon [2]. For full densification, rare-earth and alkaline earth oxides are often added as sintering aids in the fabrication of AlN ceramics [3–4]. Those properties, along with its low density (3.26 g·cm⁻³) and nontoxic characteristics, make AlN an attractive material for fabricating heat sinks and packages for microelectronic applications [5–7]. However, high sintering temperatures and long sintering time during conventional sintering are necessary for fabricating dense AlN ceramics with one sintering additive [8–10]. In contrast, spark plasma sintering (SPS) is a newly developed technique that enables ceramic powder to be fully densified at relatively low temperatures and in quite short time [11].

In the late 1970s, excellent crystallization compatibility was found between SiC and AlN by Cutler, and a complete solid solution can be formed under certain conditions [12].

The sintering activity, microstructure, mechanical properties, functional properties, and oxidation resistance of materials were largely improved with the formation of solid solutions. It is well known that the bonds between silicon and carbon atoms in SiC are very strong; consequently, SiC has a low self-diffusion coefficient. This property limits the production of high-density SiC ceramics by solid-phase sintering. To produce a high dielectric property ceramic, some SiC can be added to AlN. In this paper, low frequencies were mainly investigated to predict the high-frequency dielectric properties of AlN-SiC composite ceramics sintered by SPS at different process parameters.

2. Experiment

AlN powders with the average particle size of 2.033 μ m and nano-SiC powders with the average particle size of 40 nm were used as raw materials. The particle size distribution of AlN and a raw powder image are shown in Fig. 1. The distribution is narrow. AlN and SiC powders were wet-mixed with absolute ethanol as a dispersant by high-energy ball milling for 20 min. Then, the mixed powder was dried at 70°C for 2 h in a vacuum furnace. All tested samples were manufactured by SPS in a graphite die with an inner

Corresponding author: Cheng-chang Jia E-mail: jiachc@126.com

© University of Science and Technology Beijing and Springer-Verlag Berlin Heidelberg 2014

diameter of 20 mm.

During the SPS cycle, a vacuum of <5 Pa was maintained in the sintering chamber and the pressure of sintering was 30 MPa. Both the heating and cooling rates were 100°C/min between room temperature and 1600°C. After a holding

time of 5 min, the samples were obtained with the diameter of 20 mm and the thickness of 2.5 mm. The double faces of the samples were polished to cylinders of $\phi 20 \text{ mm} \times 2 \text{ mm}$ to ensure the consistency in subsequent measurements.

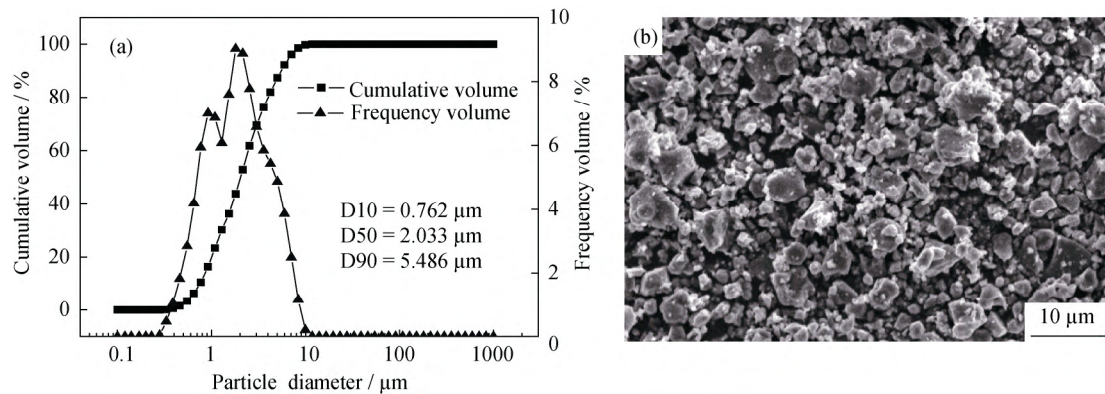


Fig. 1. Grain size distribution (a) and surface morphology (b) of aluminum nitride.

Microstructures and morphologies of the samples were examined by scanning electron microscopy (SEM). X-ray diffraction was used to identify the formed phases. Densities of the samples were measured by the Archimedes drainage method. Capacitance (C) and dielectric loss ($\tan\delta$) of the specimens at different electromagnetic frequencies were measured using an Agilent 4284 precision impedance analyzer (Agilent Technologies Japan, Ltd.). The measured electromagnetic band was from 1 kHz to 1 MHz. The permittivity (ε) was calculated by

$$\varepsilon = \frac{Ch}{\varepsilon_0 A} \quad (1)$$

where h is the thickness of the sample, ε_0 is the permittivity of vacuum, and A is the surface area of the electrode tip of the sample. The true density (ρ) was calculated by

$$\rho_{re} = \frac{\rho}{\rho_{th}} \times 100\% \quad (2)$$

where ρ_{re} is the relative density, and ρ_{th} is the theoretical density [13].

3. Results and discussion

3.1. Phase analysis

Fig. 2 shows the XRD patterns of AlN-SiC composite ceramics, which were manufactured using different amounts of SiC. The composite ceramics contained not only AlN and β -SiC but also 2H-SiC and Fe_5Si_3 . The principal crystalline phases of the sintered materials were not affected by the different amounts of SiC. Iron was introduced into AlN-SiC

composite ceramics during high-energy ball milling because of the stainless-steel mill ball and pot; then, Fe_5Si_3 was formed by the reaction of some Si and Fe atoms. Since the melting point of Fe is lower than that of AlN and SiC, AlN and SiC particles were wetted by molten Fe powder during SPS; this is conducive to densification. The crystal structures of 2H-SiC and AlN are similar, so it is easy for them to form a solid solution. According to previous reports, some 3C-SiC becomes 2H-SiC in the solid solution [14–16].

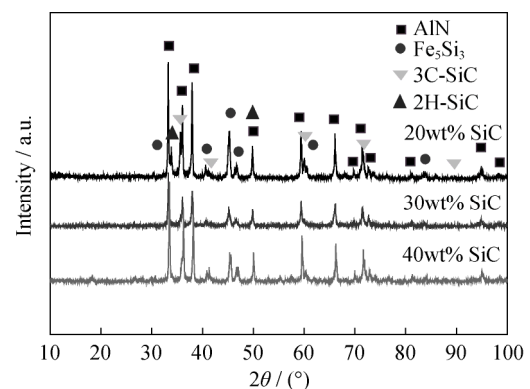


Fig. 2. XRD patterns of AlN-SiC composite ceramics.

3.2. Material density

Relative densities of the four SPS specimens ranged from 91.4% to 94.8% as the content of SiC decreased (Fig. 3). This illustrates that high-density materials can be manufactured by SPS without adding sintering aids. Increases in sintering temperature, holding time, and pressure increased the density of composite ceramics. The theoretical density can

be obtained by

$$\rho_{\text{AlN-SiC}} = \frac{1}{\frac{\omega_{\text{AlN}}}{\rho_{\text{AlN}}} + \frac{\omega_{\text{SiC}}}{\rho_{\text{SiC}}}} \quad (3)$$

where ω_{AlN} and ω_{SiC} are the mass fraction of AlN and SiC, respectively; ρ_{AlN} and ρ_{SiC} are the theoretical density of AlN and SiC, respectively.

3.3. Microstructure

All tested samples were manufactured from the mixed powders of AlN and 20wt%, 30wt%, 35wt%, 40wt% SiC. Images of the fracture morphology for AlN-SiC with different contents of SiC are shown in Fig. 4.

Based on XRD patterns for AlN-SiC in Fig. 2, Fe_5Si_3 compounds are present in the ceramic samples. Any iron that was initially distributed around pores melted to liquid

and filled the pores. Since Fe is conductive, Fe atoms contributed to the dielectric loss of the material. Fe_5Si_3 may also have some effect on attenuation properties.

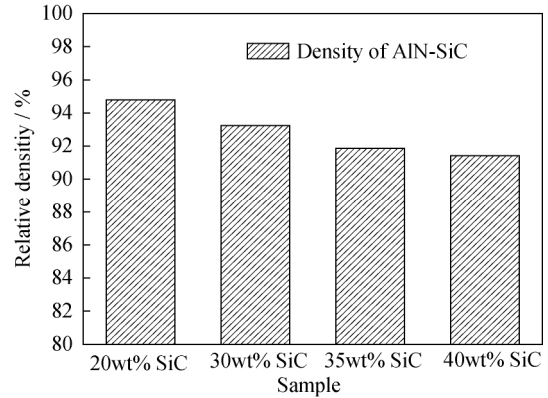


Fig. 3. Relative density of composite ceramics with different contents of SiC.

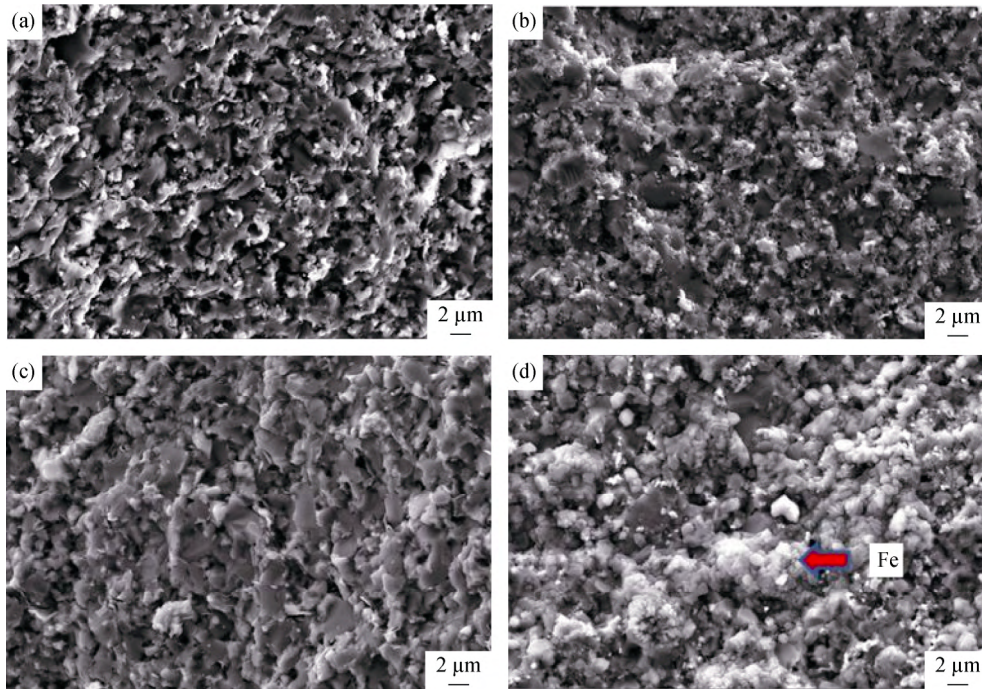


Fig. 4. Images of the fracture morphology for AlN-SiC composite ceramics with different contents of SiC: (a) 20wt%; (b) 30wt%; (c) 35wt%; (d) 40wt%.

In Fig. 4, the relatively brighter portions contain Al, Si, C, and Fe, the gray phase is the AlN substrate, and black phases are small amounts of pores. Small SiC particles were mainly present at the boundaries and pore edges of AlN grains and were substantially dispersed in the AlN substrate. Some SiC particles were located at triple-grain junctions, and their distribution was homogeneous in AlN-30wt%SiC ceramics, as shown in Fig. 4(b). Since sintering of SiC is more difficult than that of AlN, as the amount of SiC increased, the pores and dielectric loss tangent of sintered AlN

increased, as shown in Fig. 4.

3.4. Permittivity and dielectric loss at low frequency

Fig. 5 shows the dielectric properties of the ceramic samples. The permittivity and dielectric loss of AlN-SiC composite ceramics increased as the SiC content increased. However, at the same content of SiC, the dielectric loss and permittivity decreased with the increase of frequency. The dielectric loss of AlN-30wt%SiC was more than 0.3 at most frequencies from 1 kHz to 1 MHz. The dielectric loss

was significantly higher than that of a sample that was sintered with SiC powder composed of micron-size particles. Nanoscale SiC has good absorbing properties. The AlN-40wt%SiC composite ceramic had the largest dielectric

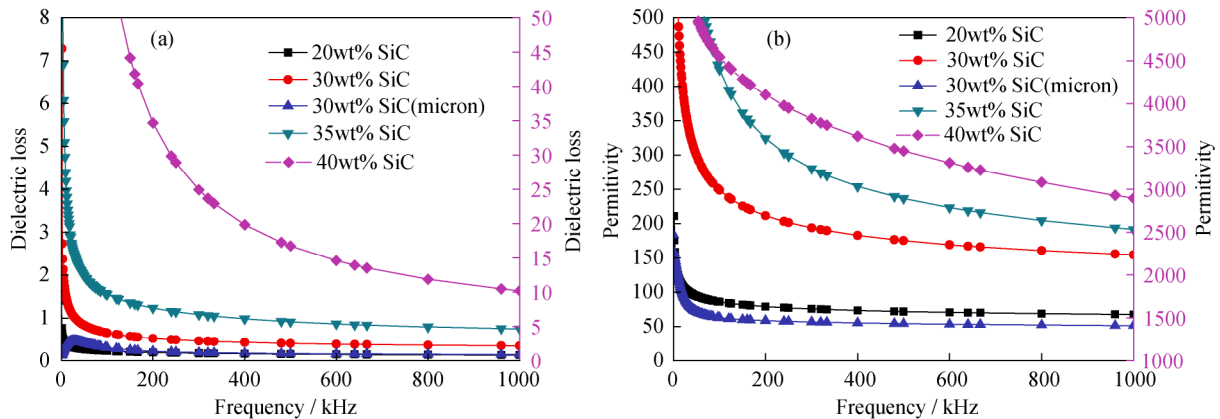


Fig. 5. Effects of SiC content on the dielectric properties of AlN-SiC composite ceramics at low frequencies: (a) dielectric loss; (b) permittivity.

3.5. Permittivity and dielectric loss at high frequency

Fig. 6 shows the frequency dependence of the complex relative permittivity (including real and imaginary parts) measured from microwave absorption studies. The real part of the permittivity is related to energy storage and the imaginary part is related to dielectric loss in the particles [17]. The figure shows that both the real and imaginary parts of the permittivity for AlN-30wt%SiC whiskers are much higher compared to those for other composites. The real part

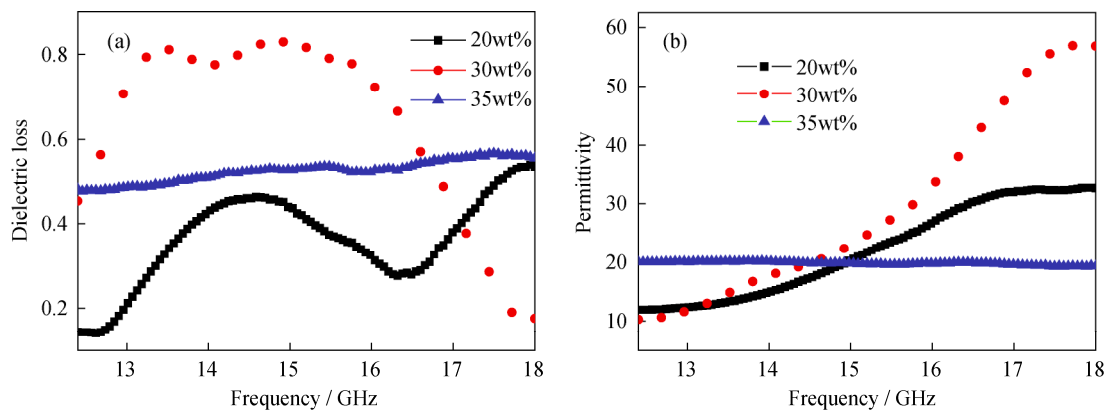


Fig. 6. Effects of SiC content on the dielectric properties of AlN-SiC composite ceramics at high frequencies: (a) dielectric loss; (b) permittivity.

Similar to a zinc-blend structure, β -SiC is composed of C and Si atoms. Si atoms are located at the center of the tetrahedron, and C atoms are at the vertices. Every pair of Si and C atoms are connected by a covalent bond. At a sintering temperature of 1600°C and pressure of 30 MPa, the surface vapor pressure of AlN powder is much larger than that of

loss and permittivity. As the SiC content increased, Fe_5Si_3 compounds were changed more and more, and may also have contributed to the attenuation properties of the materials.

(Fig. 6(b)) increases with the increase of frequency over the entire range from 12.4 to 18 GHz. The imaginary part (Fig. 6(a)) increases from 12.4 to 13.52 GHz, and is almost constant with increasing the frequency from 14.08 to 14.92 GHz, then decreases from 14.92 to 18 GHz; in other words, a resonance peak occurs at 14.92 GHz. The dielectric loss and permittivity of AlN-35wt%SiC increase very slightly with increasing the frequency from 12.4 to 18 GHz. For AlN-35wt%SiC, the dielectric loss was more than 0.48, and the stable permittivity was around 20.

SiC powder, so the evaporation rate of AlN powder is faster than that of SiC powder. Since the self-diffusion coefficient of AlN powder is higher than that of SiC powder [18], some Al atoms may dissolve into SiC lattices.

An Al atom has only three valence electrons, while an Si atom has four. If an Al atom replaces an Si atom and forms

chemical bonds with the four nearest C atoms, the compound still lacks an electron and will capture a valence electron from C, Si, or an atom of any impurities. The covalent bond of SiC crystal charges an electropositive hole. After accepting an electron, an Al atom is electronegative and becomes an Al ion. Due to electrostatic attraction, the holes are bound by Al atoms and cause thermal motion near Al atoms [19]. When external electromagnetic fields change, the Al atoms and holes can be considered to be a pair of dipoles, and dielectric polarization takes place. When the frequency of the external electric field is high enough to result in a relaxation polarization loss, the polarization time cannot keep up with the changing cycles of the external electric field. Point defects form in the solid solution of N and SiC atoms, creating a polarization current under the action of the electromagnetic field; so, the electromagnetic energy changes into other forms of energy and dissipates [20]. As the number of those defects caused by the dipoles increases, the dielectric loss and relative permittivity also increase. For a single SiC particle, dielectric loss is the absorption of the electromagnetic wave at the interior of the particle and the scattering loss of electromagnetic waves from the grain boundary. The dielectric loss of electromagnetic waves is promoted by the interface that is formed between SiC particles and the AlN matrix; this effect is stronger at the interface of nano-SiC than that of micron SiC. A large number of dangling bonds at the nanoparticle surface also causes interfacial polarization. The high specific surface area causes multiple scattering, while nano-particle electronic energy levels were split by the quantum size effect and this process consumes the energy of electromagnetic waves. In summary, dielectric loss and permittivity increase as the SiC content increases.

At low frequencies, AlN-SiC composite ceramics have conductivity losses. If we assume that AlN-SiC only has the displacement polarization of electrons and ions, the dielectric loss can be shown by the dielectric loss tangent ($\tan\delta$) (Fig. 7). As the conductive loss increases, more energy is converted to heat. The dielectric loss tangent is expressed as

$$\tan \delta = \frac{\varepsilon_r''}{\varepsilon_r'} \quad (4)$$

where ε_r'' is the real part of permittivity, and ε_r' is the imaginary part of permittivity.

4. Conclusions

(1) AlN-SiC composite ceramics were developed for applications involving electromagnetic waves from 1 kHz to 1

MHz. We found that AlN-30wt%SiC ceramics sintered by SPS at a pressure of 30 MPa and without sintering aids show a dielectric loss tangent of more than 0.3 and a relative density of more than 93%. Nano-SiC is a good microwave absorber and has strong absorbing properties.

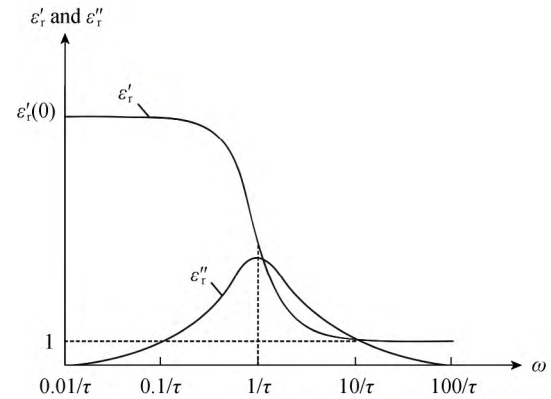


Fig. 7. Dielectric constant and dielectric loss as the functions of frequency (ω is the frequency and τ is the relaxation time).

(2) A composite containing AlN and a conductive second phase of 40wt% SiC showed better properties than those containing other contents of SiC. The composite ceramics studied here contained not only AlN and β -SiC but also 2H-SiC and Fe_5Si_3 .

(3) The microwave attenuation mechanism of AlN-SiC composite ceramics mainly involves polarization loss and conduction loss. Electromagnetic scattering influenced by various defects, interfaces, and the nano-SiC surface effect also contributes to the dielectric loss of ceramics.

Acknowledgements

This work was financially supported by the International S&T Cooperation Program of China (No. 2010DFR50360).

References

- [1] O. Sbaizero and G. Pezzotti, Residual stresses and R-curve behavior of AlN/Mo composite, *J. Eur. Ceram. Soc.*, 21(2001), No. 3, p. 269.
- [2] L. Qiao, H.P. Zhou, and R.L. Fu, Thermal conductivity of AlN ceramics sintered with CaF_2 and YF_3 , *Ceram. Int.*, 29(2003), No. 8, p. 893.
- [3] K. Komeya, H. Inoue, and A. Tsuge, Role of Y_2O_3 and SiO_2 additions in sintering of AlN, *J. Am. Ceram. Soc.*, 57(1974), No. 9, p. 411.
- [4] K. Komeya, A. Tsuge, H. Inoue, and H. Ohta, Effect of CaCO_3 addition on the sintering of AlN, *J. Mater. Sci. Lett.*, 1(1982), No. 8, p. 325.

- [5] X.L. He, F. Ye, Z.Q. Zhou, and H.J. Zhang, Thermal conductivity of spark plasma sintered AlN ceramics with multiple components sintering additive, *J. Alloys Compd.*, 496(2010), No. 1-2, p. 413.
- [6] Y. Liu, H. Zhou, L. Qiao, and Y. Wu, Low-temperature sintering of aluminum nitride with YF_3 - CaF_2 binary additive, *J. Mater. Sci. Lett.*, 18(1999), No. 9, p. 703.
- [7] J. Jarrige, K. Bouzouita, C. Doradoux, and M. Billy, A new method for fabrication of dense aluminium nitride bodies at temperatures as low as 1600°C, *J. Eur. Ceram. Soc.*, 12(1993), No. 4, p. 279.
- [8] L. Qiao, H.P. Zhou, H. Xue, and S.H. Wang, Effect of Y_2O_3 on low temperature sintering and thermal conductivity of AlN ceramics, *J. Eur. Ceram. Soc.*, 23(2003), No. 1, p. 61.
- [9] Z. Peng, Y.P. Bao, Y.N. Chen, L.K. Yang, C. Xie, and F. Zhang, Effects of calculation approaches for thermal conductivity on the simulation accuracy of billet continuous casting, *Int. J. Miner. Metall. Mater.*, 21(2014), No.1, p. 18.
- [10] H. Chen, C.C. Jia, and S.J. Li, Effect of sintering parameters on the microstructure and thermal conductivity of diamond/Cu composites prepared by high pressure and high temperature infiltration, *Int. J. Miner. Metall. Mater.*, 20(2013), No. 2, p. 180.
- [11] G. Pezzotti, A. Nakahira, and M. Tajika, Effect of extended annealing cycles on the thermal conductivity of AlN/ Y_2O_3 ceramics, *J. Eur. Ceram. Soc.*, 20(2000), No. 9, p. 1319.
- [12] M.S. Shakeri, Effect of Y_2O_3 on the crystallization kinetics of TiO_2 nucleated LAS glass for the production of nanocrystalline transparent glass ceramics, *Int. J. Miner. Metall. Mater.*, 20(2013), No. 5, p. 450.
- [13] N. Cewen, *Heterogeneous Material Physics-Microstructure-Coherent Properties*, Science Press, Beijing, 2005, p. 97.
- [14] M. Hotta and J. Hojo, Inhibition of grain growth in liquid-phase sintered SiC ceramics by AlN additive and spark plasma sintering, *J. Eur. Ceram. Soc.*, 30(2010), No. 10, p. 2117.
- [15] A. Zangvil and R. Ruh, Phase relationships in the silicon carbide-aluminum nitride system, *J. Am. Ceram. Soc.*, 71(1988), No. 10, p. 884.
- [16] M. Hotta and J. Hojo, Effect of AlN additive on densification, microstructure and strength of liquid-phase sintered SiC ceramics by spark plasma sintering, *J. Ceram. Soc. Jpn.*, 117(2009), No. 9, p. 1009.
- [17] L.D. Liu, Y.P. Duan, L.X. Ma, S.H. Liu, and Z. Yu, Microwave absorption properties of a wave-absorbing coating employing carbonyl-iron powder and carbon black, *Appl. Surf. Sci.*, 257 (2010), No. 3, p. 842.
- [18] G. Magnani, A. Brillante, I. Bilotti, L. Beaulardi, and E. Trentini, Effects of oxidation on surface stresses and mechanical properties of liquid phase pressureless-sintered SiC-AlN- Y_2O_3 ceramics, *Mater. Sci. Eng. A*, 486(2008), No. 1-2, p. 381.
- [19] F. Boey, A.I.Y. Tok, Y.C. Lam, and S.Y. Chew, On the effects of secondary phase on thermal conductivity of AlN ceramic substrates using a microstructural modeling approach, *Mater. Sci. Eng. A*, 335(2002), No. 1-2, p. 281.
- [20] T. Kusunose, T. Sekino, and K. Niihara, Production of a grain boundary phase as conducting pathway in insulating AlN ceramics, *Acta Mater.*, 55(2007), No. 18, p. 6170.